

The Cause Analysis of Valve Stem Bolt Failures in Nuclear Power Plant

Shuaishuai Song¹, Jun Qi¹, Zhankun Bai¹, Qishu Fang^{2*}

¹Mechanical Maintenance Department, Shandong Nuclear Power Co.,Ltd., Haiyang, Shandong 216600, China

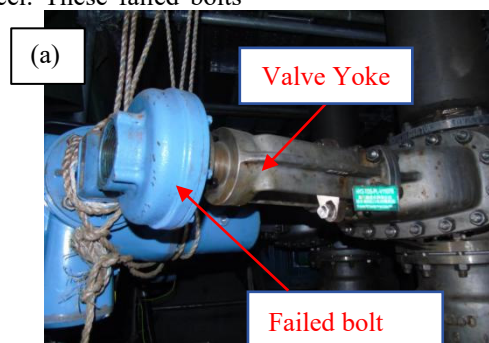
²SPIC Power Station Operation Technology (Beijing) Co.,Ltd., Beijing 112209, China

Abstract: The shaft of the electric isolation valve at the outlet of the seawater tank pump in a nuclear power plant fractured due to bolt failure, resulting in detachment and loss of electrical switching function. Upon disassembly, it was discovered that all connecting bolts on the frame were fractured. Macroscopic examination, chemical composition analysis, hardness testing, metallographic examination, scanning electron microscope (SEM) observation, and energy spectrum analysis were performed on the fractured bolts. Results revealed significant deviation from design specifications for stainless steel austenite in terms of their chemical composition; instead they consisted of low-alloy steel (40Cr). High-strength bolts exposed to marine environments are susceptible to corrosion-induced stress cracking or hydrogen embrittlement leading to fracture. Replacement is recommended as a preventive measure against corrosion-induced bolt failure.

1. Introduction

The shaft of the electric isolation valve's actuator connected to the frame of the electric head on the condenser intake side of a nuclear power plant broke, causing the actuator to separate from the frame, rendering the valve unable to operate electrically. A more extensive inspection was conducted on similar valves from the same manufacturer, revealing that multiple identical types of valves had issues with the bolts connecting the actuator to the frame, severely damaging the internal valve stem nut and thrust bearing of the electric actuator. The failed bolts were made of A193-B8M austenitic stainless steel. These failed bolts

were located above the seawater pool in the underground level -14m of the conventional island of the nuclear power plant, operating in a humid marine environment. Since the pump upstream of the valve was started every 5-7 hours, the same valve had to be frequently switched on and off within the same time interval. The threaded connection was used to secure the yoke frame, with the threaded bolt passing through the hole from below and connecting to the threaded hole above to secure the yoke frame and electric actuator. Once these bolts failed, it would affect the safe operation of the valve and prevent the system from functioning normally. Figure 1 shows the location of the failed bolt and the macro morphology of the partial failure bolt sample.



*Corresponding author's e-mail address: fangqishu820726@163.com



Figure 1. Overall macroscopic photo of the fractured bolt (numbered 1-5 in sequence)
(a) The failed part of the bolts in the valve; (b) Sample of partially failed bolts.

2. Experiments and results

2.1. Visual inspection

Among them, the base material of Bolt No. 5 had been seriously corroded, and the clear thread pattern was no longer obvious. The middle thread surface had also suffered mechanical damage, which was probably caused during cutting. In contrast, the right thread was

relatively intact and had less corrosion products attached to it, which might be because they were in the hole position. By analyzing the macroscopic fracture surface, it was found that a layer of gray-black corrosion products covered the fracture surface. The fracture surface was even or stepped, without obvious necking, showing typical brittle fracture characteristics. Figure 2 shows the macroscopic morphology of Bolt No. 5



Figure 2. Macroscopic morphology of No. 5 fractured bolt
(a)transversely fractured bolts; (b) axially cracked bolts

2.2. Chemical compositions

This study used the ASTM E415 standard test method and employed an ARL 3460 type spectrometer for flame atomic emission spectrometry. The results of the bolt base material analysis are shown in Table 1, it was found that the No. 4 broken bolt samples taken were not consistent with the material specified in the drawing

(A193M-B8M), and there was a significant difference. According to the actual situation, these bolts belong to low-alloy steel (40Cr), rather than austenitic stainless steel, and contain the anti-pitting element Mo. According to the comparison with GB/T3098.1-2010 standard, its chemical composition is closer to the carbon steel grade 12.9 and 9.8 with added elements.

Table 1 Chemical composition of bolts (mass fraction,%)

Elements	C	Si	Mn	P	S	Cr	Ni	Mo	Cu
No. 4	0.40	0.23	0.63	0.016	<0.010	1.00	<0.010	0.035	0.041
B8M	≤0.08	≤1.00	≤2.00	≤0.045	≤0.030	16.0~18.0	10.0~14.0	2.00~4.00	/
40Cr	0.37~0.44	0.17~0.37	0.50~0.80	≤0.020	≤0.010	0.80~1.10	≤0.30	≤0.10	≤0.25
Grade 12.9	0.28~0.50	/	/	≤0.025	≤0.025	/	/	/	/
Grade 9.8	0.15~0.40	/	/	≤0.025	≤0.025	/	/	/	/

*ASTM A193/A193M: Standard Specification for Alloy-Steel and Stainless Steel Bolting Materials for High-Temperature Service.

2.3. Hardness test

According to the test method specified in ASTM E92 standard, a 430MVA Vickers hardness tester is used to measure the Vickers hardness HV10 of the metal material surface with a 10 kg load. The cross-sectional hardness of the 1-5 bolts was tested. The results showed

that the hardness values of bolts 1-4 were 414-417 HV, while the hardness value of bolt 5 was 315 HV. According to the requirements of grade 12.9 and grade 9.8 specified in GB/T 3098.1-2010 standard, the hardness range should be between 385-435 HV and 290-360 HV, respectively. Furthermore, after converting the tensile strength using the GB/T 1172-1999 standard

for black metal hardness and strength conversion values, it was found that the tensile strength of bolts 1-4 exceeded 1300 MPa, while the tensile strength of bolt 5

was 1028 MPa. The specific hardness values are shown in Table 2.[1-2]

Table 2. Hardness test results of bolts (hardness, HV10) and Tensile strength conversion value

hardness	1	2	3	mean value	Tensile strength conversion value (MPa)
1	414	417	414	415	1332
2	414	416	418	416	1335
3	414	415	413	414	1328
4	418	414	418	417	1338
5	316	314	315	315	1028
B8M			≤321		≤1047
Grade 12.9			385~435		≥1220
Grade 9.8			290~360		≥900

2.4. Metallographic examination

Microstructural analysis was conducted on the cross-section of the bolt bolt fracture, and the longitudinal section was examined for non-metallic inclusions using an OLYMPUS GX71 optical microscope. Through metallographic observation, it was found that the base material of the bolt had a tempered martensite microstructure, while the thread surface had a

large number of randomly distributed corrosion pits of various sizes, as shown in Figure 3. According to GB/T 10561-2005, "Standard Rating Chart for Determining the Amount of Non-metallic Inclusions in Steel by Microscopic Examination," we analyzed the non-metallic inclusions in the sample, and the results showed that all the non-metallic inclusions in the sample belonged to the fine system and were rated as A1.5 and D1.5, as shown in Figure 4.

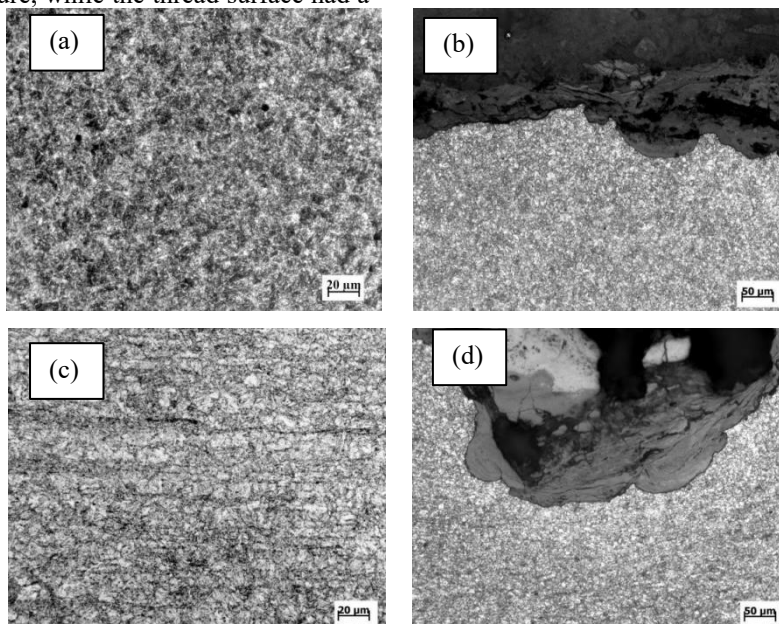


Figure 3 Microstructural Analysis of Bolt Thread Root No. 5, showing (a) Area A at 500x magnification; (b) Area B at 200x magnification; (c) Area C at 500x magnification; and (d) Area D at 200x magnification.



Figure 4 Non-metallic Inclusion Evaluation of Bolt No. 5

2.5. Microstructural Analysis of Fracture Surfaces

The fracture surface morphology of No. 5 sheared bolt was studied by using GeminiSEM 300 field emission scanning electron microscope., as shown in Figure 5. Combining the macroscopic analysis of the fracture surface, it can be known that a layer of gray-black corrosion products covers the fracture surface, and the fracture surface cannot be seen clearly before cleaning. The overall fracture surface presents a ductile dimple characteristic, indicating a ductile fracture.

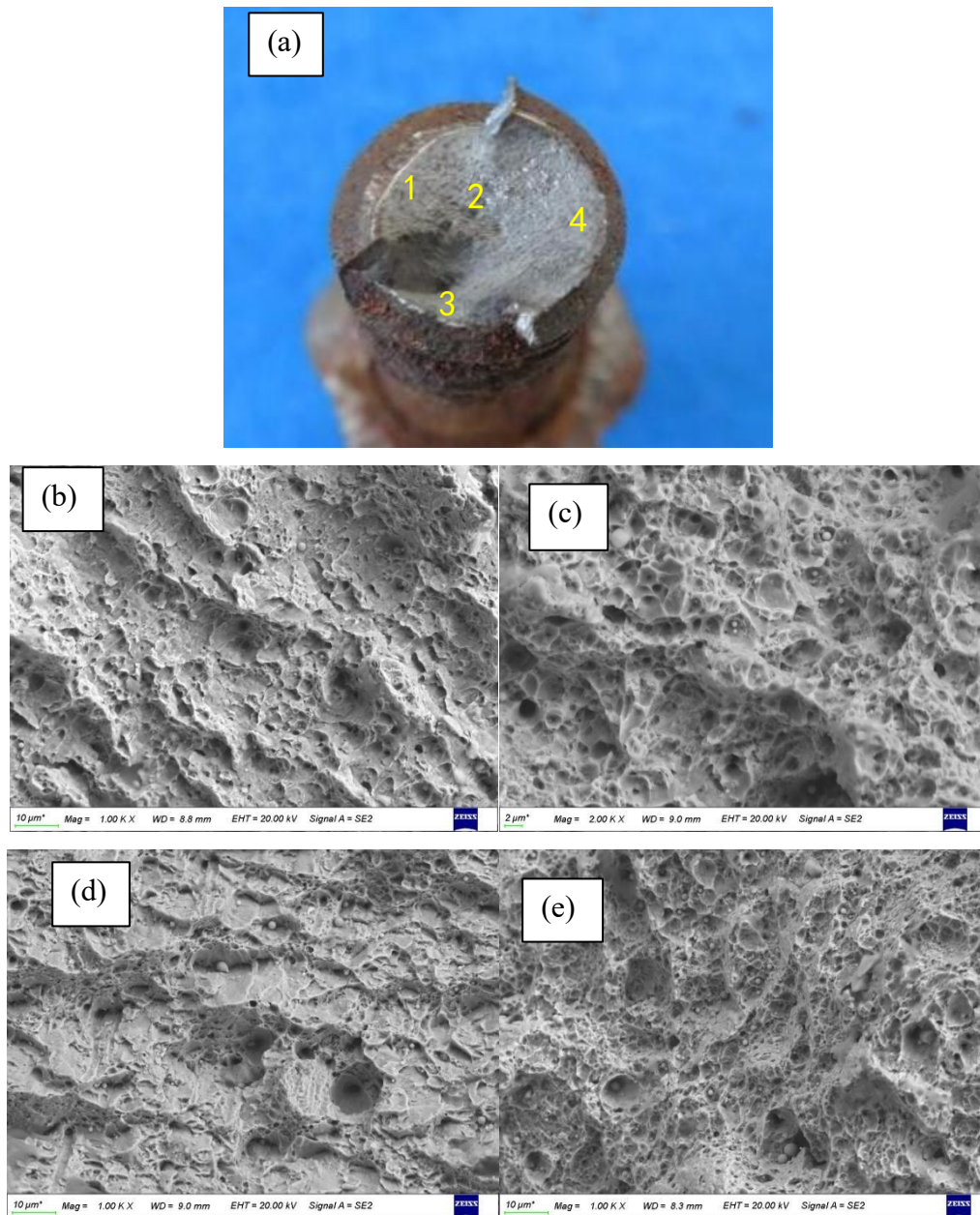


Figure 5 Illustrates the microscopic morphology of the bolt fracture surface, showing (a) the overall morphology; (b) microscopic morphology at Position 1; (c) microscopic morphology at Position 2; (d) microscopic morphology at Position 3; and (e) microscopic morphology at Position 4.

2.6. Energy dispersive spectrometry analysis

After conducting EDS analysis through GeminiSEM 300 field emission scanning electron microscope, we observed that the microstructural surface of the 1st

broken bolt joint was covered with a large amount of corrosion products, mainly composed of Fe oxides. According to the results of the spectrum shown in Figure 6, these corrosion products contain common elements in seawater such as Cl, Ca, and Na.

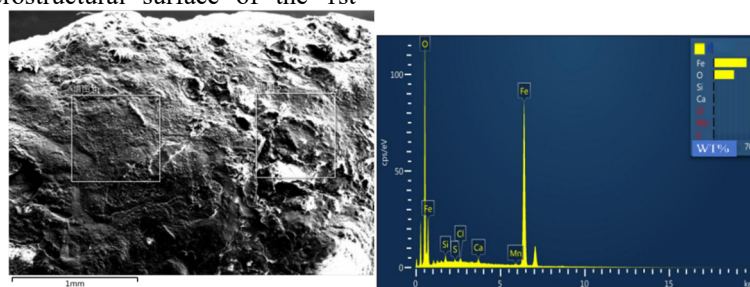


Figure 6 EDS analysis of the bolt fracture surface
(a) Microstructure of the fracture surface; (b) EDS analysis results of the local area.

3. Analysis and discussion

Based on the results of comprehensive physical and chemical testing, the chemical composition of the bolt material does not conform to the specifications in A193M-B8M drawing, and there is a significant difference. The A193M-B8M material used in the original design was an austenitic stainless steel containing Mo for resistance to sea water corrosion, while the actual material used was a low-alloy steel (40Cr). The results of the energy spectrum analysis show that the corrosion products contain Cl, Ca, and Na, which are marine elements, indicating that the bolt has been corroded by the marine environment[3-5].

The fracture surface of Bolt No. 5 shows a ductile dendrite feature, indicating a ductile fracture type, indicating that the bolt was subjected to a significant force before failure. The location of the failure is above the sea water pool on the intake side of the condenser, exposed to the marine environment. The material is a low-alloy steel (40Cr), with its main alloying element being Cr, with a content of about 1%. Due to its high strength (reaching 1300 MPa and 1000 MPa respectively), it belongs to high-strength steel materials, which are prone to corrosion and stress corrosion cracking or environmental hydrogen-induced fatigue in marine environments[6-10].

4. Suggestions

- The chemical composition of the bolt material does not conform to the specifications outlined in drawing A193M-B8M; instead, it is composed of low-alloy steel (40Cr). Based on the chemical composition and hardness analysis following GB/T 3098.1-2010 standard, bolts 1-4 can be classified as grade 12.9, while the fifth bolt can be classified as grade 9.8.
- The failed bolts are high-strength bolts and are in a marine atmosphere environment. In a marine atmosphere environment, high-strength bolts are prone to corrosion, which can lead to stress corrosion cracking or environmental hydrogen-induced failure.
- It is recommended to replace the existing bolts with A193M-B8M material that meets the requirements specified in the drawing to prevent failure due to corrosion.

Reference

1. Zhao, H., Wang, P., & Li, J. 2021 International Journal of Hydrogen Energy, 46, 34983-34997.
2. Zhao, H., Li, W., Hu, P., Fu, H., & Li, J. 2022 Metallurgical and Materials Transactions A, 53, 861-873.
3. Lai, Y., Ma, Q., Zuo, D., Zhang, G., Liao, K., & Zhang, Z. 2021 In Journal of Physics: Conference Series, 2083, 022064).

4. Li, S., Lai, Y., Yang, L., & Liu, X. 2024 In Journal of Physics: Conference Series 2691, 012008.
5. Burgess, B. 2021 The APPEA Journal, 61, 77-82.
6. Wang, H., Tang, F., Qin, S., Tu, K., & Guo, J. 2020 Journal of Materials in Civil Engineering, 32, 04020203.
7. Wu, S., Zhang, Z., Chen, J., Yao, Y., & Li, D. 2023 Engineering Failure Analysis, 150, 107292.
8. Wu, S., Li, J., Guo, J., Shi, G., Gu, Q., & Lu, C. 2020 Materials Science and Engineering: A, 769, 138479.
9. Acri, A., Beretta, S., Bolzoni, F., Colombo, C., & Vergani, L. M. 2020 Engineering Failure Analysis, 109, 104330.
10. Gong, P., Turk, A., Nutter, J., Yu, F., Wynne, B., Rivera-Diaz-del-Castillo, P., & Rainforth, W. M. 2022 Acta Materialia, 223, 117488.